Final Report 'RACORO Aerosol Data Processing' P.I.: Elisabeth Andrews
Project#1547483,
Award number: DE-SC0005008

The RACORO aerosol data (cloud condensation nuclei (CCN), condensation nuclei (CN) and aerosol size distributions) need further processing to be useful for model evaluation (e.g., GCM droplet nucleation parameterizations) and other investigations. These tasks include:

(1) Identification and flagging of 'splash' contaminated Twin Otter aerosol data.
(2) Calculation of actual supersaturation (SS) values in the two CCN columns flown on the Twin Otter.
(3) Interpolation of CCN spectra from SGP and Twin Otter to 0.2% SS.
(4) Process data for spatial variability studies.
(5) Provide calculated light scattering from measured aerosol size distributions.

Below we first briefly describe the measurements and then describe the results of several data processing tasks that which have been completed, paving the way for the scientific analyses for which the campaign was designed. The end result of this research will be several aerosol data sets which can be used to achieve some of the goals of the RACORO mission including the enhanced understanding of cloud-aerosol interactions and improved cloud simulations in climate models.

During RACORO, instruments on the Twin Otter measured aerosol size distribution (using both a scanning mobility particle spectrometer (SMPS) and a passive cavity aerosol spectrometer probe (PCASP)), aerosol total number concentration (using condensation nuclei counters (CNC)), cloud condensation nuclei (CCN) concentration at various supersaturations (SS, using a two column CCN counter, CCNC), and various external parameters (e.g., altitude, ambient relative humidity, wind speed, etc). Here we utilize the Twin Otter data to address the 5 tasks listed above. Details for aerosol instrumentation used here are provided in Table 1 for both the Twin Otter and the SGP surface site.

Table 1 Details of relevant aerosol instruments on the Twin Otter and at SGP

Instrument	**Principal Investigator**	**Diameter range or <u>set-point</u> super-saturation**	**Data frequency**	**Manufacturer**
Twin Otter				
SMPS	D. Collins	0.012 - 0.58 μm	~1 min	Texas A&M
PCASP	H. Jonsson/ R. Wood	0.1 <PCASP< 1.8 μm	1 sec	PMS
CNC	H. Jonsson/ R. Wood	>0.01 μm (CPC1)	1 sec	TSI (mod#3010)
CCNC (2 column)	H. Jonsson/ R. Wood	Col. 1: 0.2<SS<1.0 Col. 2: SS~0.2	27 min scan 1 sec	DMT
SGP surface site				
SMPS	D. Collins	0.012 – 0.75 μm	Variable[1]	Texas A&M

			~45 min	
CNC	A. Jefferson	>0.01 μm	1-min	TSI (mod#3010)
CCNC (1 column)	A. Jefferson	0.15<SS<1.15	1 h scan	DMT

[1]data obtained from DOE

(1) Evaluation of splash contamination when the Twin Otter was in cloud

Prior to scientific analysis of the RACORO data set, potential problems with the data need to be identified and removed or flagged depending on the issue. The major issue identified in preliminary data review was the possibility of droplet splash affecting measured number concentrations. In a previous field campaign (CHAPS) splash artifacts were seen in CN concentrations when the DOE G1 flew through cloud. There it was hypothesized that cloud droplets entered the aerosol inlet and shattered. The fragmented droplets then dried out during transport to the instruments and the remaining droplet kernel was then sampled by the aerosol instrumentation resulting in spikes in number concentration. On historical note, Haf Jonsson noted:

> *"Many years ago a famous scientist noticed an increase in CN count every time we were in clouds and claimed a discovery of inside-cloud nucleation. It lasted about two weeks, before he himself had to admit to a splashing artifact. By then we had collected the greatest and best dataset on the artifact ever."*

In the PCASP data set there were obvious cloud contamination events where number concentrations in the larger size bins (D>0.7 μm) increased when the Twin Otter was sampling in cloud. The PCASP was wing-mounted and thus when the airplane was in-cloud the PCASP was in-cloud with a relatively short distance between cloud and measurement volume. In the DMA and CPC there was not an obvious increase in particle concentration while the Twin Otter was in cloud, nor was there an increase in CN spikes in-cloud which was how the splash artifact manifested during the CHAPS campaign These instruments were located inside the airplane and sampled off a different inlet. The DMA had a longer averaging time than the PCASP and it is also possible that the splash bits were too large to be seen by the DMA. H. Jonsson recommended LWC>0.1 xx as an indicator of the Twin Otter being in-cloud and the data potentially affected by splash. Additionally particle volume measurements from the forward scattering spectrometer probe (FSSP) and cloud-aerosol spectrometer (CAS) (both of which measure in the diameter range ~0.5-50 um) can be used to identify when large particles – likely cloud droplets are present. LWC and particle volume values from these two instruments are included in the files generated by this work to provide severaloptions in cloud screening the data.

(2) Calculation of actual SS values for the two airborne CCN columns

The first step in this analysis is to calculate the true super-saturations at which the CCN operated. The CCN 'cabin' files archived in the RACORO database contain the CCN concentrations and instrument set-point SS values estimated from various instrument settings and calibration information. However, when the CCN is operated at conditions other than for what it was calibrated (e.g., different pressures) the actual SS can be

significantly different than the set-point SS. We have used a detailed model of the instrument (Lance et al., 2006) to calculate the actual SS using the CCN 'housekeeping' data files (these files were obtained from H. Jonsson as they are not included in the RACORO archive). Figure 1 shows a representative example of the difference between calculated and set-point SS for one of the flights. At the lowest set-point (SS=0.2) the actual SS values were relatively close to the setpoint (within 0.05 SS), while at the higher set point values there was a much larger difference (a difference of almost 0.3 SS at set-point SS of 0.8). The primary cause of the differences between setpoint and actual SS were due to differences in ambient pressure from the pressure at which the CCN was calibrated.

(3) Interpolation of CCN spectra from SGP and Twin Otter to 0.2% SS

The second step in this analysis is to calculate the CCN concentration and activation diameter at SS= 0.2. We will use SS=0.2 as the primary basis for comparison with surface measurements and for investigating questions about variability in CCN properties. The constant SS CCN column set-point was SS=0.2, but as Figure 1 shows the actual SS was usually slightly different than 0.2. There are several options for adjusting to SS=0.2: (a) ignore adjustment as actual is within 0.05 SS; (b) use the CCN scans aboard the Twin Otter to do an adjustment (c) use the CCN scans from the SGP surface site to do an adjustment. While (a) is the simplest option SS in this range are often where much of the change in activation happens so a small difference in SS can make a big difference in CCN concentration. Below we discuss options (b) and (c).

One option for adjusting the values for this column would be to fit a power law relationship (equation 1) to data from the scanning CCN column on the Twin Otter::

$$(1)\quad N_{CCN} = C*SS^{k}$$

where N_{CCN} is the CCN concentration, SS is the super-saturation and C and k are fit parameters [e.g. Pruppacher and Klett, 1980]. Figure 2 shows examples of the power law fit to the data.

Figure 2 shows both a flight when the power law fitting worked really well (March 18) and one where it did not work so well (June 23). The main difference between these two flights was the pattern flown by the Twin Otter and the resulting aerosol variability. The March 18 flight was a 'surface albedo' flight and the airplane flew two patterns at 500 m above ground level (agl). Although there was some variability in the total aerosol concentration (as indicated by the CN concentration in the black triangles) this did not appear to affect the power law fit. In contrast, the June 23 flight had highly variable CN concentrations due to the pattern flown, resulting in quite poor power law fits. This was a cloud triangle flight including a spiral from high to low altitude, several triangular legs below, in, and above cloud, followed by another spiral. This suggests the Twin Otter CCN power law fits can only be used under certain ideal conditions. The adjustments to SS=0.2 cannot be applied to the constant column data without further analysis of the fits. Thus option (c) - utilizing a climatological value from the SGP surface site CCN data – may be the best choice.

Instead of using the Twin Otter power law fits to the CCN data, fits to the CCN data from the SGP surface site can be used. The advantage of the surface CCN instrument is that it typically is not subject to abrupt changes in conditions resulting in more consistent fits. The disadvantage is the necessary assumption that the power law fits derived from aerosol particles sampled at the surface are applicable aloft. In addition to spatial variability, there are temporal differences to consider as well – for simplicity a climatological average of the power law fit to the SGP data for the entire RACORO campaign period is what we will use.

The fit adjustment of Twin Otter data from the constant SS column to SS=0.2 would look like this:

$$(2)\ N_{CCN\_TO,SS=0.2} = N_{CCN\_TO,SSact} * (N_{CCN\_SGP,SS=0.2}/N_{CCN\_SGP,SSact})$$

where $N_{CCN\_TO,SS=0.2}$ is the Twin Otter CCN concentration at SS=0.2, $N_{CCN\_TO,SSact}$ is the Twin Otter CCN concentration at the actual SS, and $N_{CCN\_SGP,SS=0.2}$ and $N_{CCN\_SGP,SSact}$ are the same but for SGP. Substituting in equation 1 results in:

$$(3)\ N_{CCN\_TO,SS=0.2} = N_{CCN\_TO,SSact} * (0.2/SSact)^{k}$$

The climatological value for k (i.e., the median value of k derived from power law fits to the hourly CCN scans between Feb 11 – June 30, 2009) is 0.731. The 25th and 75th percentiles for k for this time period are 0.558 and 0.894 respectively. (Note: RACORO research flights started on Feb 8 but the CCN instrument at the surface was out of commission prior to Feb 11.) In general this adjustment resulted in a less than 10% change to the Twin Otter CCN concentrations. With the measurement supersaturations aligned with reality some scientific analyses can be performed as described below. Some of these analyses are included in Vogelmann et al. [2011].

3.1 Analyses: Calculation of activation diameter and investigation of variability

The Twin Otter data set can be used to characterize the CCN activity (e.g., activation diameter, CCN spectra, etc) of the aerosol measured aloft which can then be compared with results for a similar suite of instruments operated at the SGP surface site. This is the first step in assessing the extent to which the long-term record of surface aerosol properties at SGP can be combined with remote sensing data (updraft velocity) to predict cloud droplet number concentrations (e.g., McComiskey et al, 2009). The activation diameter is the dry diameter of the smallest aerosol particle that activates (nucleates a cloud droplet) at a particular supersaturation. To calculate the activation diameter for the aerosols observed during RACORO, we assumed that all particles have the same composition. We then added up the particle concentrations in the SMPS size bins from largest to smallest bin. The activation diameter is the middle of the size bin when the cumulative number concentration from the SMPS equals the CCN concentration at SS=0.2. Figure 3 shows this schematically. The calculation of activation diameter was done for each flight and for the SGP surface site data set. Here we use only the SMPS data to avoid the potentially confounding effects of splash. Note however, that when the

Twin Otter was flying in clear sky conditions the PCASP and SMPS provided quite similar results in terms of activation diameter.

Despite the very large differences in aerosol size distribution and CN and CCN concentration, the activation diameter tends to vary very little, both within individual flights and among all flights flown. Calculated activation diameter at the surface was also quite invariable. Figure 4a,b shows size distribution contour plots for the two flights in Figure 2 with the calculated activation diameter overlaid. Figure 4c shows a similar contour plot for the surface data for (almost) the entire RACORO campaign time period.

Figure 5 shows the observed variability in activation diameter, CCN concentration and CN concentration for both the SGP surface site and the Twin Otter flights. The median activation diameters for the entire time range are quite similar at the SGP surface site (0.16 μm) and on the Twin Otter (0.14 μm). One question is whether the larger activation diameter at SGP is related to the larger maximum bin diameter of the surface SMPS (0.75 μm) compared to that of the SMPS on the Twin Otter (0.58 μm). Counting backwards from the 0.58 μm bin at the surface does not result in any discernible change in the activation diameter statistics (not shown) so the differences in maximum bin diameter are unlikely to be the explanation for the larger activation diameters observed at the surface.

Segmenting the Twin Otter data based on whether the airplane was below (BC), in (IC) or above (AC) cloud shows that statistically there is very little difference in activation diameter (the AC segments may have a slightly lower diameter). In contrast, there are large differences (between a factor of 2 and a factor of 10) in the number concentration of CCN and CN for BC, IC and AC conditions. The below cloud segments had the highest concentrations of CN and CCN while the lowest concentrations were observed for the above cloud segments. It is not shown in a figure, but the Twin Otter data were also segmented solely on LWC values (as opposed to flight segments) for LWC > 0.02, 0.05, 0.1, 0.2, 0.3 and 0.4. There is a clear decrease in the number of CN and CCN at all percentile levels for LWC>0.02 compared to values for the entire data set and the decrease in number concentration is greater at higher LWC. In contrast the activation diameter gets more variable at higher LWC, with both decreases in value for the lower percentiles and increases for the upper percentiles.

3.2 Analyses: Estimation of CCN solubility

At SS=0.2 a pure ammonium sulfate particle will activate at ~0.09 um dry diameter. The median activation diameter at SS=0.2 calculated from the Twin Otter measurements during RACORO was ~0.14 um. One possible explanation is that the composition of particles sampled during RACORO cannot be represented by pure ammonium sulfate. The presence of insoluble material in a particle increases the activation diameter for a given supersaturation compared to the diameter at which a particle of pure ammonium sulfate would activate (Seinfeld and Pandis, 1998, pp 790-793). Figure 6 shows the critical supersaturation as a function of particle diameter for different contents of insoluble material mixed with ammonium sulfate. The vertical green lines represent the extremes (5^{th} and 95^{th} percentiles) and median values of activation diameter observed on

the Twin Otter at SS=0.2. At SS=0.2, the vertical diameter lines intersect solubility lines where the soluble material ranges from 10-50% of the particle – in other words, this suggests that the particles are 50-90% insoluble material (median 80% insoluble). This is consistent with filter measurements of sub-um aerosol mass and major ions concentration made by PMEL suggest the unidentified mass (total mass – sum(major ions mass)) at SGP is 58% +/- 14% of the total mass.

3.3 Analyses: Variation of activation diameter and CCN with CN concentration

CCN form on the existing CN population. The size and composition of the CN particles determine how many particles will activate to CCN and what the activation diameter would be for a given SS. Here we look at the relationships between activation diameter, CN and CCN number concentration at SS=0.2 to see if we can gain any simple insights; specifically we address the following questions:

(1) How does activation diameter change with increasing CN concentration? Komppula et al. 2005 studied this at a remote site in northern Finland. They found higher activation diameters for polluted air masses than for clean arctic air masses. This suggests changes in aerosol chemistry at higher CN concentrations due to differences source regions or atmospheric processing during transport.

(2) What is the relationship between CCN concentration and activation diameter?

(3) How does CCN concentration correlate with CN concentration?

In general CCN concentration is expected to increase with CN concentration. The relationship can change due to external factors (e.g., updraft velocities [e.g, Feingold, 2003]) or internal factors (e.g., CN size distribution, composition, mixing state [Ervens et al., 2007]). As the CCN measurements described here are made by activating aerosol within the controlled conditions of the DMT CCN instrument, external factors such as updraft velocity or ambient supersaturation are not a factor - observed changes in the relationship between CCN and CN will be connected to differences in aerosol properties.

Figure 7 shows population density plots of activation diameter plotted against CCN and CN number concentration and CCN concentration plotted against CN concentration for the Twin Otter and SGP. For both sites, there is no definite trend for activation diameter as a function of CN concentration. For the TO data there's a hint that activation diameter may increase with CN number concentration as was seen by Komppula et al., 2005, but the surface data at SGP don't suggest this trend. The range of activation diameters is smaller at SGP - there few cases with activation diameters ($dp<0.1\ \mu m$) are observed. The plots of activation diameter versus CCN concentration for both the Twin Otter and SGP show a slight (very slight) indication of decreasing activation diameter with increasing CCN. CCN concentrations increase in the presence of more CN, but there is not a tight relationship between the two. On the Twin Otter, CCN concentrations appear to cluster into at least two groups as a function of CN concentration. The first group lies closer to the y-axis on the plot with CCN/CN = 0.4 while the second group lies closer to the x-axis on the plot with CCN/CN = 0.02. At the surface the CCN concentration falls between the CCN/CN=0.02 and CCN/CN=0.4 lines. As mentioned above, external

factors such as updraft velocity or ambient supersaturation are not responsible for the range in CCN/CN observed here. Instead, aerosol properties such as size and/or chemistry are controlling the activation to CCN. Chemistry data are not available for this data set and analysis of the effect of changes in size distribution on CCN activation has not been done (yet!).

The Twin Otter data can be segregated based on various parameters (e.g., altitude or humidity) to determine if certain conditions control which group (group 1 – CCN/CN~0.4; CCN/CN~0.02) the points will fall in. Points in group 1 tend to be sampled at high altitude and have a lower activation diameter. Points sampled during high LWC (>0.04) tend to also fall into group 1 rather than group 2, although at low LWC (<0.02) points fall in both groups. Similarly, points sampled when the wind direction was more northerly (300<WD<90) are typically in group 1. Southerly winds tend to encompass most of the points in group 2 but also include points in group 1. At higher relative humidity more points tend to be in group 1 and vice versa. There is also one cluster of points in group 1 that appears to be different than the rest of group 1. These are the points where CCN concentration > ~700 cm^{-3}. These points appear to correspond to southerly winds and low altitude.

Based on the simple segregation done above, a cluster analysis can be used to determine if there are distinct grouping patterns for CCN/CN. Figure 8 shows a simple cluster analysis where the Twin Otter data were clustered on altitude and wind direction. The black points represent the entire data set and the colored points represent the points in each cluster. The plots are ordered by increasing median altitude. The WD value in the upper right corner of each plot is the cosine of the wind direction angle, so southerly winds correspond to negative numbers and northerly winds to positive numbers. The first two plots (Figure 8ab) are low altitude (<1 km) clusters. Figure 8a has a median wind direction from the north and is dominated by points in group 2, while Figure 8b has a median wind from the south. Figure 8b contains the points in the subset of group 1 mentioned above. Figures 8cd show the mid-altitude (between 1-2 km) clusters. The middle altitude plot with the northerly wind (Figure 8c) tends to file fall primarily in group 1 while the other mid-altitude plot encompasses both groups. Figure 8ef show the high altitude (>2 km) clusters and most of the points fall into group 1 for both plots. To summarize the cluster results northerly winds and higher altitudes tend to be associated with lower CN concentration and higher CCN/CN ratios, i.e., closer to CCN/CN~0.4 while southerly winds and low altitudes are correlated with higher CN concentrations but lower activation fractions, i.e., closer to CCN/CN~0.2. This suggests there are differences in the aerosol properties (chemistry/size) as a function of altitude and/or source region. The next step is to look at whether there are significant differences in the aerosol size distribution that might explain this. (since don't have chemistry).

3.4 Comparison of CCN VAP with CCN concentration estimated from DMT CCN measurements at SS=0.2

On a side note, Don Collins at Texas A&M developed a 'Value Added Product' (VAP) to calculate CCN concentration as a function of SS using humidified tandem differential mobility analyzer (HTDMA) measurements. Figure 9 shows a time series and a scatter

plot of the CCN concentration at SS=0.1998 (i.e., approximately SS=0.2) calculated from the VAP with CCN concentration at SS=0.2 estimated from the fits to the CCN counter scans. The time series shows that the two values track each other quite nicely. The scatterplot shows that there is a decent relationship between the two estimates of CCN concentration (R2=0.68) which is quite remarkable given the values are based on measurements from different instruments and derived using different techniques.

(4) Spatial variability of aerosol

Understanding the spatial variability of aerosol allows for comparisons of data on different time and spatial scales. It can be useful for validation of remote sensing instruments because often space-based measurements are not exactly co-located with the ground-based validation platform. The spatial variability analysis helps explain differences that might be expected with time/distance. Another application occurs when comparing model output to point measurements (e.g., in-situ measurements at a surface monitoring site). It is typically assumed that the point measurement should be representative of the model grid box values but those grid boxes can be quite large (100s km) and not reflect the spatial variability observed at the site.

Anderson et al. [2003] presented work challenging the concept that aerosol concentration and chemistry vary on the synoptic scale (e.g., order of 1000 km) but are generally invariant within an air mass. They utilized three different types of data (1) in-situ aerosol scattering measurements at two surface sites (Bondville, Il and Spitzbergen, Sweden (2) airborne in-situ aerosol scattering measurements obtained during long (24-648 km) level flight legs in the ACE-Asia campaign and (3) space borne lidar extinction measurements from a lidar carried on the space shuttle during the Lidar In Space Experiment (LITE). Their analysis suggested aerosol varied on the mesoscale (40-400 km) rather than synoptic scale. The scale of variability at the sites they studied was in the range of ~100 km or ~5 h (assuming an advection velocity of 20 km/h). They attributed the observed mesoscale variability to the local-to-regional nature of aerosol sources and sinks.

Targino et al. [2005] followed the methodology of Anderson et al [2003] for aerosol measured during ACE-2. They found the spatial scales of variability (based on light scattering) to be 3-8 km which is more than an order of magnitude lower than what Anderson et al [2003] reported. Targino et al. suggested that this could be real difference due to air masses types sampled, location of the study or perhaps because their study used shorter (117-244 km) flight segments than were used by Anderson et al. [2003].

There were four flights during RACORO which included long (115-250 km), straight, level flight legs intended for assessing spatial variability of the aerosol. These flights occurred on April 20, May 30, May 31 and June 1 of the RACORO campaign. Each flight had 2 legs which could be used in the analysis. The start and end times for each of the legs were identified using either the information in the flight log or, in the case of April 20, changes in the heading of the Twin Otter. Unlike the Anderson et al. [2003] and Targino et al. [2005] efforts, light scattering was not measured on the Twin Otter during RACORO. Here we use CN concentration and PCASP volume concentration to investigate spatial variability during these four flights. (We do not use scattering from

DMA because of low time resolution of that data.) There were no clouds reported during any of these flights, thus issues of splash affecting the PCASP data are not applicable. We also looked at variability of the aerosol optical properties at the surface SGP site to compare with what was measured aloft.

In this analysis we observed different lag correlations depending on which variable was investigated. PCASP concentrations (dp > 0.1 um) tended to have high spatial variability (very short lag correlation time, on order of minutes) similar to what Targino et al. [2005] found for airborne scattering variability.. CPC concentrations (dp > 0.01 um) tended to have the less spatial variability (1-8 h) more like what was found by Anderson et al. [2003] for scattering, It is difficult to directly compare our estimates of the variability of aerosol number concentration with the literature values, since both Targino et al. [2005] and Anderson et al. [2003] looked at variability of aerosol scattering rather than particle concentration. At the surface we found that the surface measurements have a time scale of 2-5 h for CN, absorption and scattering. The time scales observed at the surface SGP for scattering are similar to what Anderson et al. [2003] found for the sites they studied.

(5) Calculation of light scattering from size distribution measurements

Optical properties calculated from size distributions using Mie theory can be used for comparison and evaluation of remote sensing instruments such as aerosol lidar and sun photometers, as well as with in-situ optical measurements made at the surface at SGP. Here we have calculated aerosol optical properties from DMA and PCASP size distribution measurements assuming a refractive index (RI) of 1.55 + 0.015i. This RI was used to obtain closure between calculated and measured aerosol scattering during the 2003 IOP at the SGP surface site (Andrews et al., 2006). The aerosol optical properties (absorption, total scattering, back-scattering and asymmetry parameter) were calculated at four wavelengths (450, 550 and 700 nm were chosen to match TSI nephelometer measurements at the surface and 532 nm is the wavelength of the HSRL measurements). Ångström exponents for several of the wavelength pairs were also calculated. Files containing these calculated values have been uploaded to the ARM IOP data archive for use by the scientific community.

It should be noted that the calculated absorption is VERY questionable as it strongly depends on the assumed imaginary part of the refractive index which is not well defined. Furthermore, the Mie code used in these calculations (Wiscombe, 1980) assumes homogeneous spherical particles and may not appropriately represent the characteristics of the absorbing aerosol. That said, in their closure study, using the same methodology and assumed RI, Andrews et al., (2006) showed reasonable agreement between calculated light absorption and light absorption measured by a co-located particle soot absorption photometer (PSAP) (within 3% on the basis of the slope of a line forced through the origin, $R^2 = 0.43$). Here we have no absorption measurements to compare with as an absorption instrument was not part of the Twin Otter payload.

Figure 10 presents a comparison of vertical profiles of aerosol loading from three flights in June 2009. The aerosol scattering calculated from DMA and PCASP size distributions is plotted along with the extinction derived from HSRL scans and measured surface

aerosol scattering over each Twin Otter flight. The DMA and PCASP scattering profiles were calculated at 532 nm to match the HSRL wavelength. The calculated scattering was further adjusted to ambient humidity based on the June climatology of aerosol hygroscopicity measurements at the surface. In general there is quite good agreement between the calculated scattering and extinction. There tends to be some noise in the PCASP measurements at higher ambient humidity (RH>90%), perhaps due to influence of cloud.

(6) Conclusions and future work

Tasks 1,2,3 involved cleaning up the CCN data so that it can be used for model evaluation (e.g., GCM droplet nucleation parameterizations) and other investigations. Initial results obtained following this clean-up have been included in Vogelmann et al [2011]. Future work relating to these tasks is that of making available to the wider science community files for each flight with the correct CCN, SS and CN data. These files exist and merely need to be reformatted and uploaded to the ARM IOP site. This will happen by the end of 2011. Task 4 – spatial variablility results suggest that the airborne aerosol CN concentration has similar variability to that observed at the SGP site and also is similar to the variability for scattering reported by by Anderson et al. [2003] for several different surface and airborne data sets. Future work should include calculating variability for calculated scattering from the PCASP (e.g., from task 5) aboard the Twin Otter so that the results are more directly comparable to the Anderson et al. [2003] and Targino et al. [2005] findings. Finally data files containing calculated aerosol optical parameters for various wavelengths have been generated. We envision these being of use to the HSRL science team for comparison/validation of HSRL aerosol profiles with values of extinction and angstrom exponent. Another possible use is with comparison/evaluation of the lidar measurements at the SGP surface site.

Figure 1 Actual and setpoint super-saturation values for May 8 (DOY=128) flight. Top pane is scanning SS column (column A), bottom pane is constant SS column (column B). Black lines are set-point SS, red lines are SS calculated using Lance et al. (2006) model.

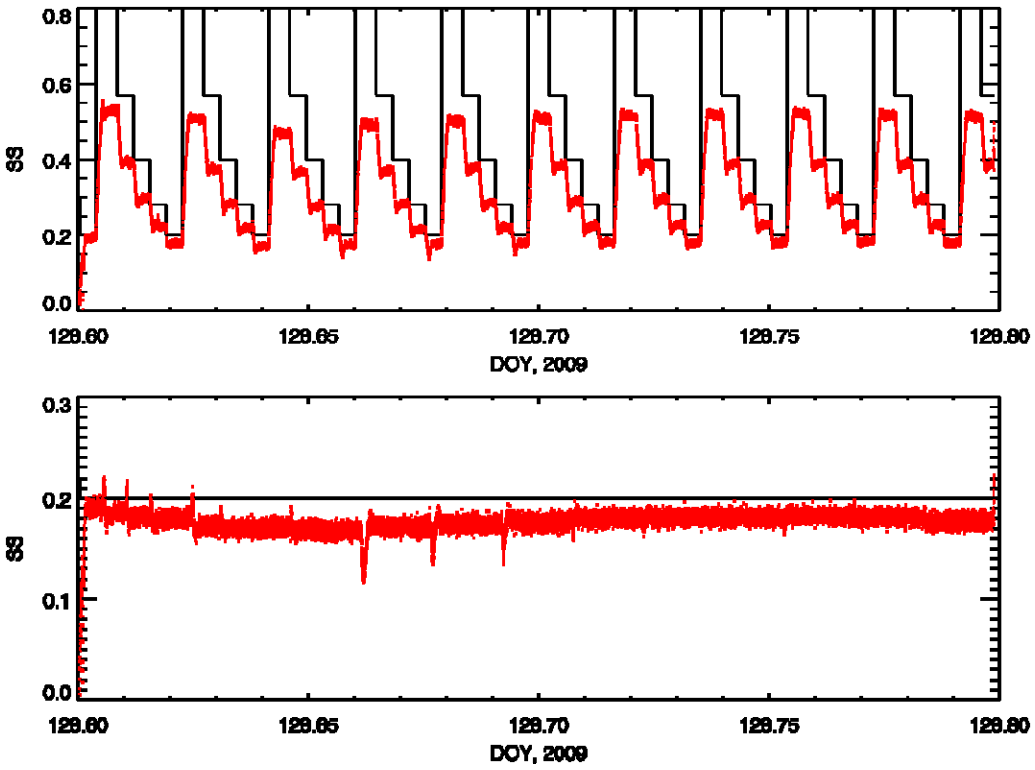

Figure 2 Example of time series of power law fits, top pane March 18 (DOY 77), bottom pane June 23 (DOY 174). Black triangles are CN concentration, red triangles are measured CCN concentration and purple dots are CCN concentration calculated using the power law fit parameters.

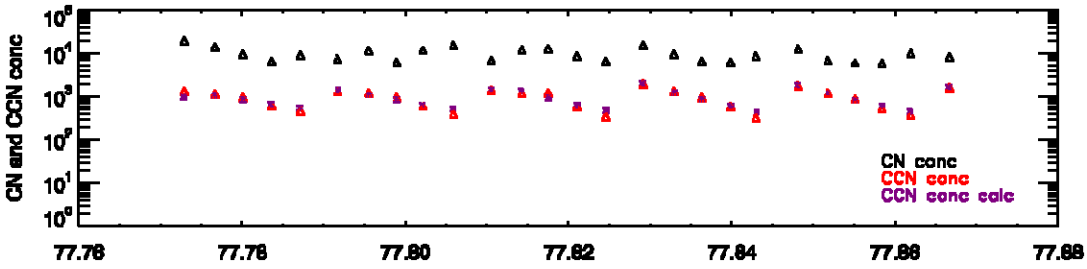

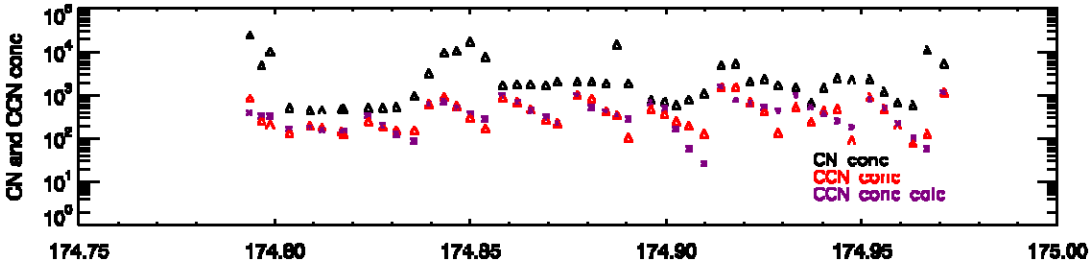

Figure 3 Schematic of activation diameter calculation. Black numbers are number in each bin, blue numbers are cumulative number added from largest to smallest bin.

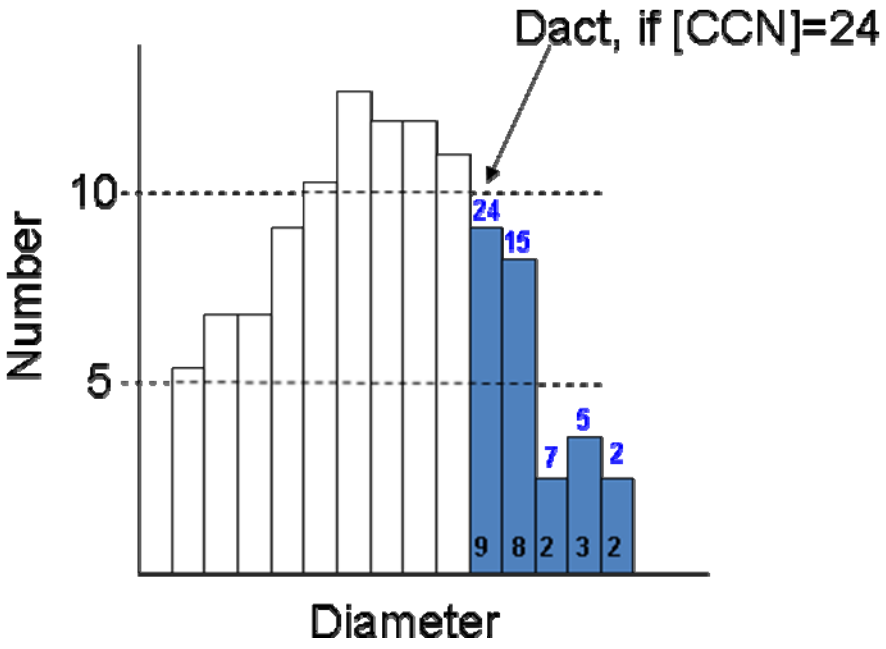

Figure 4 Contour plots of aerosol size distributions overlaid with calculated activation diameter. Top pane (a) Twin Otter - March 18 (DOY 77); middle pane (b) Twin Otter - June 23 (DOY 174); bottom pane (c) SGP – Feb 11 – June 30

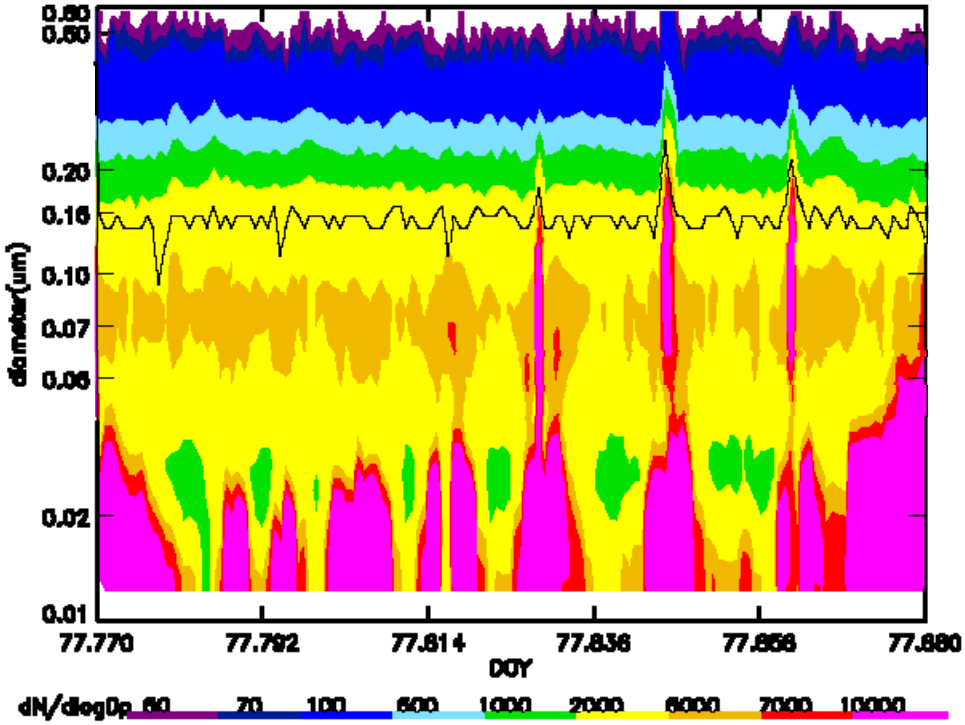

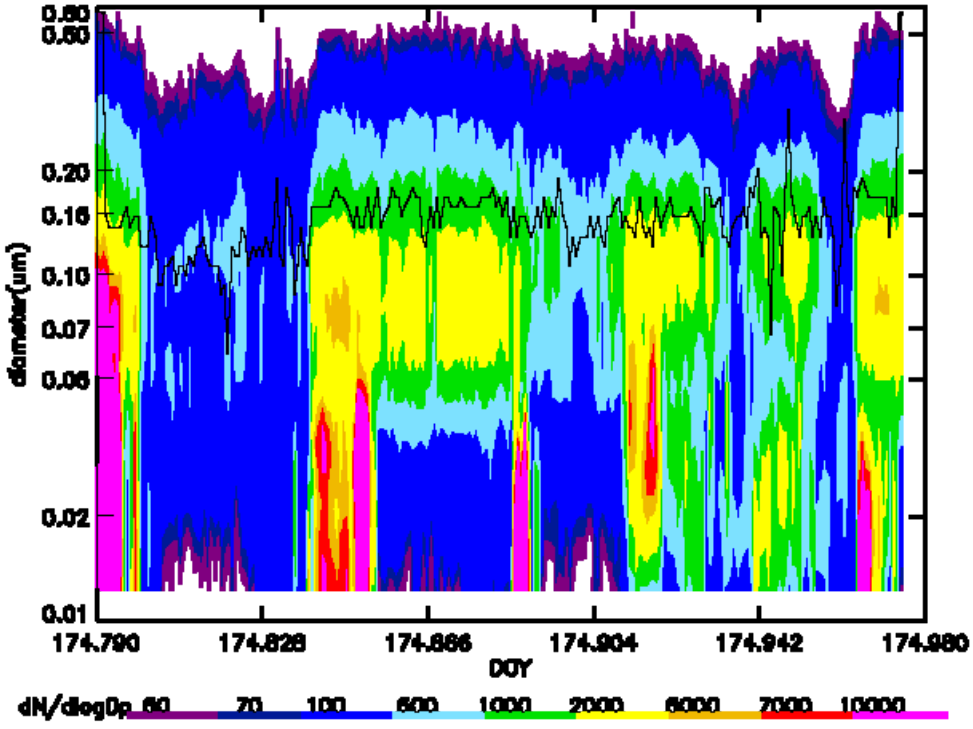

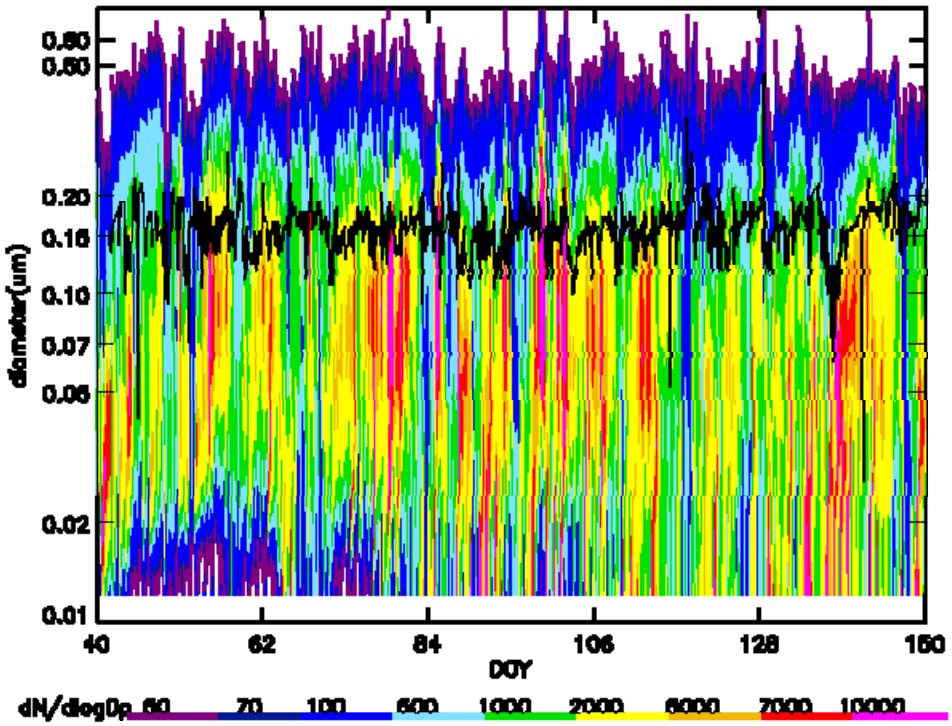

Figure 5 Box-whisker plots of variability of calculated activation diameter at SS=0.2, CCN concentration at SS=0.2 and CN concentration for SGP (red) and various sub-sets of the Twin Otter data (yellow). The 'all' category includes the entire Twin Otter dataset; the BC subset includes data from segments identified as 'below cloud' triangles, turbulence legs, clear sky aerosol triangles, aerosol variability long-legs and surface albedo flights (regardless of altitude). The 'IC' subset includes the entire 'in-cloud' triangle even if parts of triangle were not in cloud. The 'AC' sub-set includes the entire 'above cloud' triangle even if parts of the triangle were skimming the cloud tops. Percentiles depicted are: 5th, 25th, 50th, 75th, 95th.

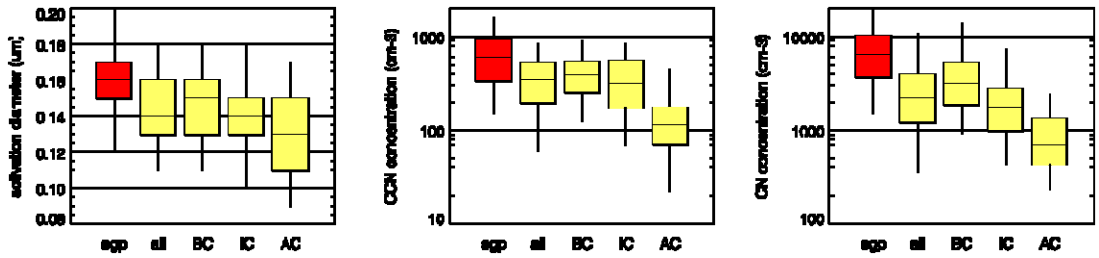

Figure 6 Critical supersaturation as a function of particle diameter for different contents of insoluble material mixed with ammonium sulfate.

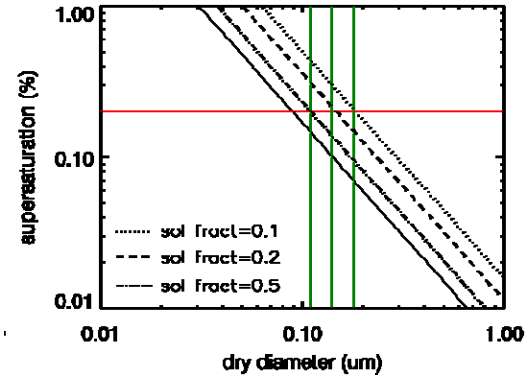

Figure 7 Relationship between activation diameter, CCN and CN on Twin Otter (top three plots) and at SGP surface site (bottom three plots). The red lines show the CCN/CN=0.4 and CCN/CN=0.02 in both plots. Note the different axes for TO and SGP data.

Twin Otter

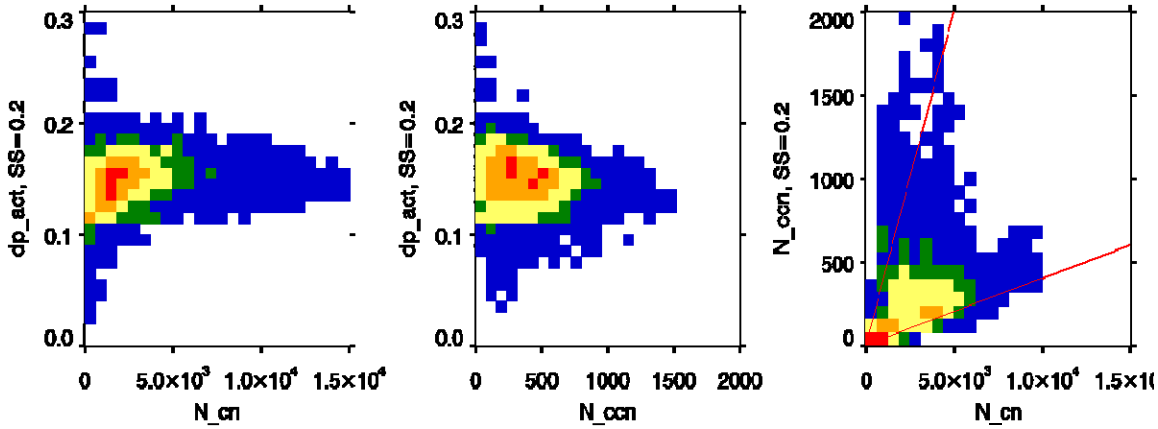

SGP

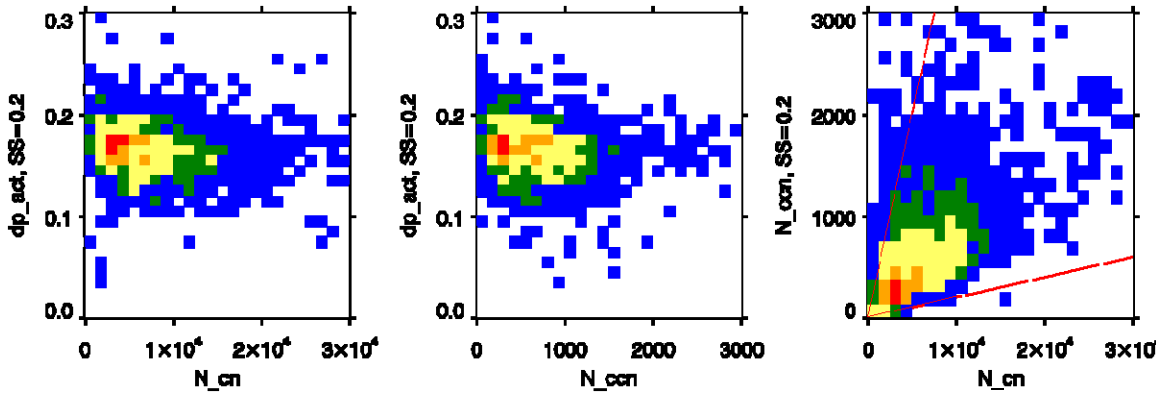

Figure 8 Cluster analysis of Twin Otter data on altitude and wind direction

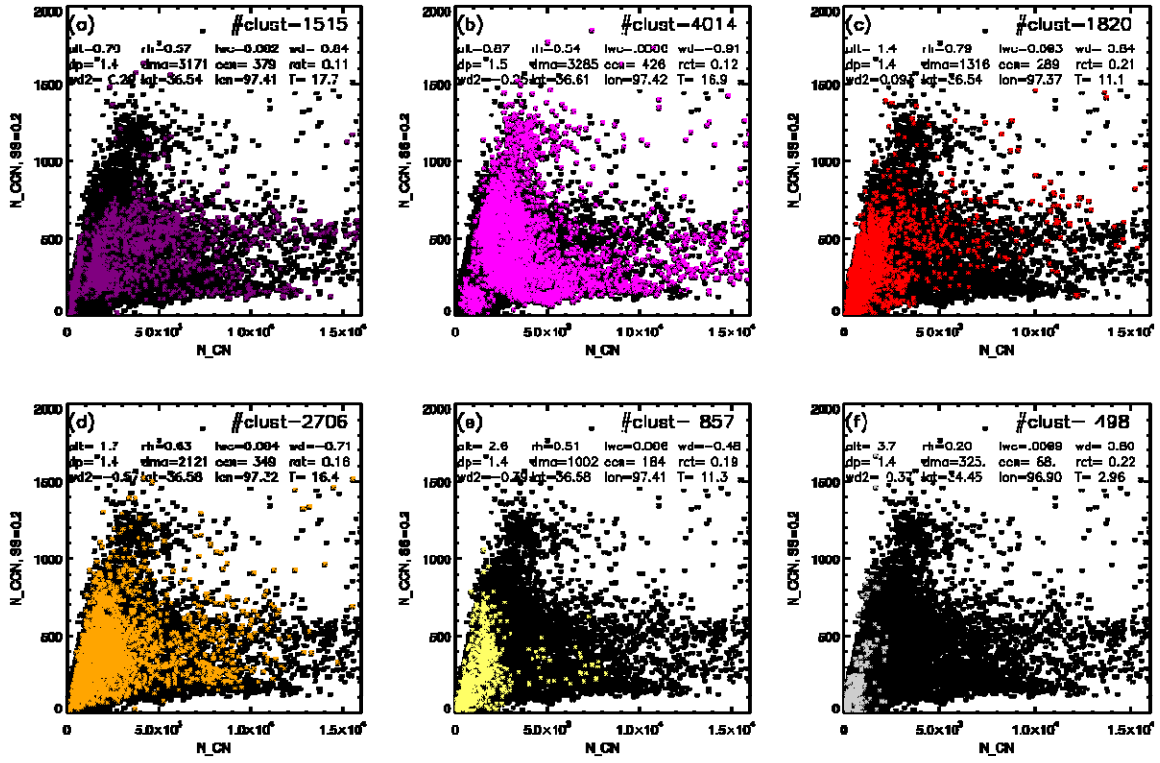

Figure 9 comparison of CCN concentrations at SS=0.2 from the DMT CCN counter and from the VAP utilizing HTDMA measurements. Top plot shows time series, bottom plots shows scatter plot with 1:1 line in red and fit in blue.

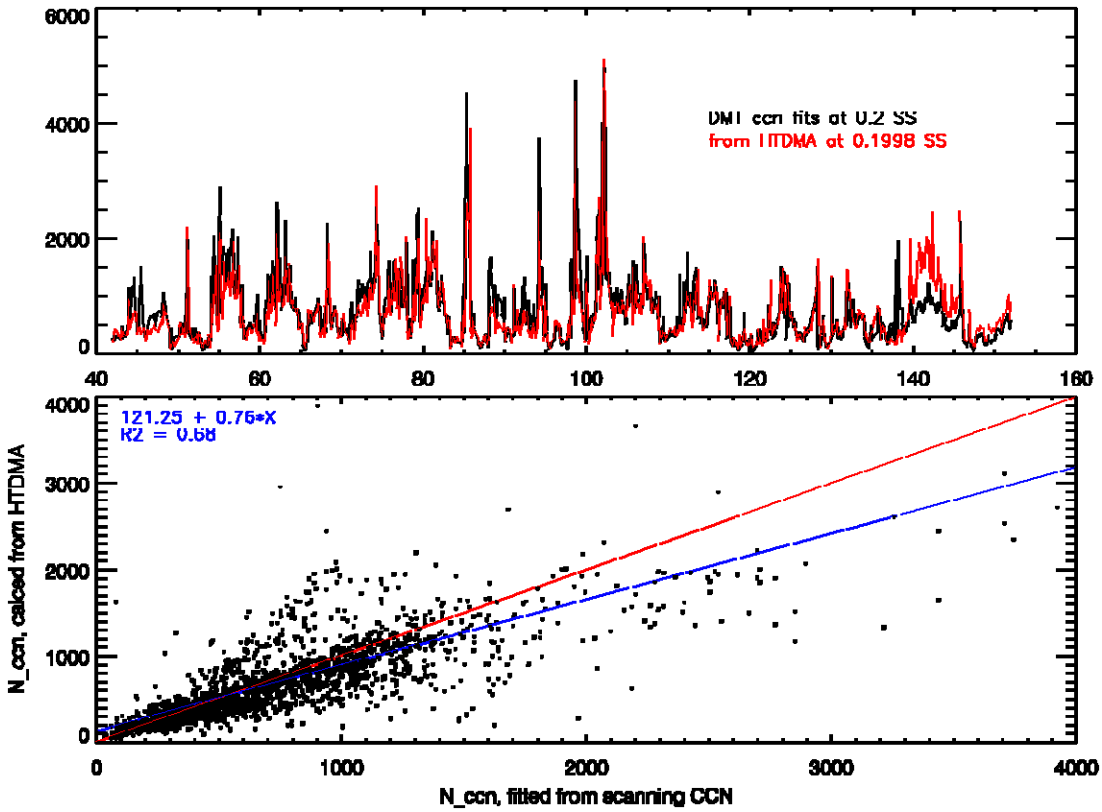

Figure 10 shows comparisons of calculated aerosol scattering profiles with HSRL extinction profiles and with surface aerosol scattering during the time of the Twin Otter profile. Profiles are for June 8, June 17 and June 23, respectively.

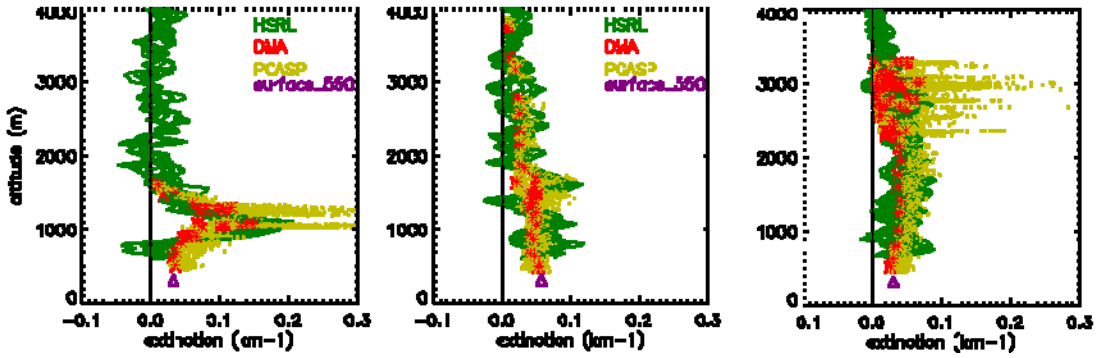

References

Anderson, T.L, Charlson, R.J., Winker, D.M., Ogren, J.A., Holmen, K., "Mesoscale Variations of Tropospheric Aerosols" J. Atmos. Sci., 60, 119-136, 2003.

Andrews, E., Sheridan, P.J., Fiebig, M., McComiskey, M., Ogren, J. A., Arnott, P., Covert, D., Elleman, R., Gasparini, R., Collins, D., Jonsson, H., Schmid, B., Wang., J., Comparison of methods for deriving aerosol asymmetry parameter J. Geophys. Res., Vol. 111, No. D5, D05S04, doi:10.1029/2004JD005734, 2006.

Ervens, B Cubison, M Andrews, E Feingold, G Ogren, JA Jimenez, JL; DeCarlo, P Nenes, A, 'Prediction of cloud condensation nucleus number concentration using measurements of aerosol size distributions and composition and light scattering enhancement due to humidity,' J. Geophys. Res., 112, D10, D10S32, doi: 10.1029/2006JD007426, 2007

Feingold G., 'Modeling of the first indirect effect: Analysis of measurement requirements,' Geophys. Res. Lett., 30(19), 1997, doi: 10.1029/2003GL017967, 2003

Komppula M; Lihavainen H; Kerminen VM; et al., 'Measurements of cloud droplet activation of aerosol particles at a clean subarctic background site,' J. Geophys. Res., 110, D6, D06204, doi: 10.1029/2004JD005200, 2005.

Lance, S Medina, J., Smith, JN Nenes, A., 'Mapping the operation of the DMT Continuous Flow CCN counter,' Aerosol Sci. Technol., 40(4), 242-254, 2006.

McComiskey A.; Feingold G.; Frisch A. S.; et al.,' An assessment of aerosol-cloud interactions in marine stratus clouds based on surface remote sensing,' J. Geophys. Res., 114, D09203, doi: 10.1029/2008JD011006, 2009

Targino, A.C., Noone, K.J., Ostrom, E., "Airborne *in situ* characterization of dry aerosol optical properties in a multisource influenced marine region" Tellus, 57B, 247–260, 2005.

Wiscombe, W. J., Improved Mie scattering algorithms, Appl. Optics, 19, 1505-1509, 1980.

Pruppacher, H.R. and Klett, J.D., Microphysics of Clouds and Precipitation, D. Reidel Publishing Co., Boston, 1980 (page 226).

Vogelmann, A.M. et al., "RACORO Extended-Term, Aircraft Observations of Boundary-Layer Clouds," submitted to Bull. Amer. Meteor. Society. Aug. 2011.